Article

High contribution of non-fossil sources to sub-micron organic aerosols in Beijing, China

Yanlin Zhang, Hong Ren, Yele Sun, Fang Cao, Yunhua Chang, Shoudong Liu, Xuhui Lee, Konstantinos Agrios, Kimitaka Kawamura, Di Liu, Lujie Ren, Wei Du, Zifa Wang, Andre S.H. Prevot, Soenke Szidat, and Pingqing Fu

Environ. Sci. Technol., **Just Accepted Manuscript** • DOI: 10.1021/acs.est.7b01517 • Publication Date (Web): 24 Jun 2017

High contribution of non-fossil sources to sub-micron organic aerosols in Beijing, China

Yanlin Zhang[1]*, Hong Ren[2,8], Yele Sun[2,8], Fang Cao[1], Yunhua Chang[1], Shoudong Liu[1], Xuhui Lee[1,9], Konstantinos Agrios[3,4], Kimitaka Kawamura[5], Di Liu[6], Lujie Ren[7], Wei Du[2,8], Zifa Wang[2], André S.H. Prévôt[4], Sönke Szidat[3], Pingqing Fu[2,7,8]*

[1] Yale-NUIST Center on Atmospheric Environment, Nanjing University of Information Science and Technology, Nanjing 210044, China

[2] LAPC, Institute of Atmospheric Physics, Chinese Academy of Sciences, Beijing 100029, China

[3] Department of Chemistry and Biochemistry & Oeschger Centre for Climate Change Research, University of Bern, Bern 3012, Switzerland

[4] Paul Scherrer Institute (PSI), Villigen-PSI 5232, Switzerland

[5] Institute of Low Temperature Science, Hokkaido University, Sapporo 060-0819, Japan

[6] School of Geography, Earth and Environmental Sciences, University of Birmingham, Birmingham, B15 2TT, United Kingdom

[7] Institute of Surface-Earth System Science, Tianjin University, Tianjin 300072, China

[8] College of Earth Sciences, University of Chinese Academy of Sciences, Beijing 100049, China

[9]School of Forestry and Environmental Studies, Yale University, New Haven, CT, USA

[*]*Corresponding authors*. E-mails: dryanlinzhang@outlook.com or zhangyanlin@nuist.edu.cn (Y. Zhang) and fupingqing@mail.iap.ac.cn (P. Fu)

Phone: +86 25 5873 1022; fax: +86 25 5873 1193

Abstract

Source apportionment of organic carbon (OC) and elemental carbon (EC) from PM1 (particulate matter with a diameter equal to or smaller than 1 μm) in Beijing, China was carried out using radiocarbon (^{14}C) measurement. Despite a dominant fossil-fuel contribution to EC due to large emissions from traffic and coal combustion, non-fossil sources are dominant contributors of OC in Beijing throughout the year except during the winter. Primary emission was the most important contributor to fossil-fuel derived OC for all seasons. A clear seasonal trend was found for biomass-burning contribution to OC with the highest in autumn and spring, followed by winter and summer. ^{14}C results were also integrated with those from positive matrix factorization (PMF) of organic aerosols from aerosol mass spectrometer (AMS) measurements during winter and spring. The results suggest that the fossil-derived

primary OC was dominated by coal combustion emissions whereas secondary OC was mostly from fossil-fuel emissions. Taken together with previous ^{14}C studies in Asia, Europe and USA, a ubiquity and dominance of non-fossil contribution to OC aerosols is identified not only in rural/background/remote regions but also in urban regions, which may be explained by cooking contributions, regional transportation or local emissions of seasonal-dependent biomass burning emission. In addition, biogenic and biomass burning derived SOA may be further enhanced by un-resolved atmospheric processes.

TOC

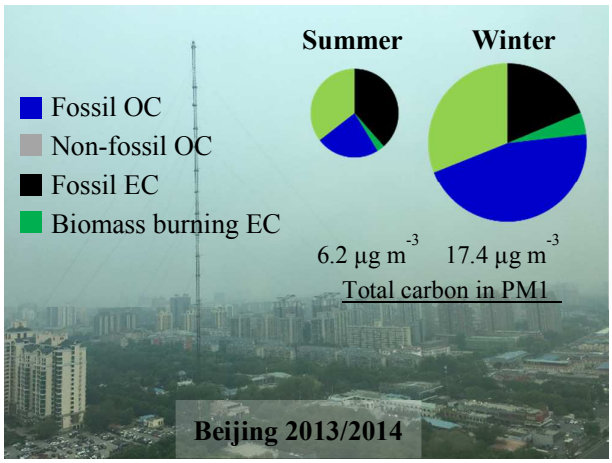

1 Introduction

Carbonaceous aerosols, which can contribute 20-90% of the total fine aerosol mass concentrations [1, 2] are of great importance due to their significant and complex impacts on air quality, human health and climate [3-5]. According to different physical and chemical properties, bulk carbonaceous aerosols (total carbon, TC) are operationally divided into two sub-fractions namely organic carbon (OC) and elemental carbon (EC) or black carbon (BC) when carbonate carbon (CC) may be negligible or less than 5% of the TC mass in fine (i.e. PM2.5, particulate matter with a diameter equal to or smaller than 2.5 μm) or sub-micron particulate matter (PM1) [6]. PM1 may be more important to human health compared to PM2.5 because smaller particles may have higher ability to penetrate into the human respiratory system [7]. OC can scatter or reflect solar light leading to a net cooling effect on the Earth' climate, whereas EC can significantly contribute to global warming due to its light absorbing behavior [5]. OC and EC not only differ in their chemical and environmental effects but also differ in their origins and formation [6, 8]. OC can be emitted as primary OC (POC) and formed as secondary OC (SOC) through gas-to-particle conversion after gas-phase oxidation of volatile organic precursors or aqueous-phase processing of low-molecular-weight water-soluble organic compounds [6, 8-10]. EC almost exclusively originates from incomplete combustion either from fossil-fuel combustion or biomass burning [11]. POC and its precursors can be emitted from fossil (e.g., coal combustion and vehicle exhaust) and non-fossil sources (e.g., biomass burning, vegetation emissions, cooking) [8, 12-14]. Several studies have revealed that OC and EC differ in

their origins and formation processes based on bottom-up and top-down approaches [15-18], and it is therefore very challenging to quantitatively determine contributions from different sources to OC and EC separately, especially in polluted urban regions.

Beijing, the capital of China, is one of largest megacities in the world with a population of 20 million over an area of 16 800 km^2 and it has faced serious air pollution problems for the last decades. Zheng et al. (2015) found that PM2.5 is associated with an average total mortality of 5100 individuals per year for the period 2001–2012 in Beijing, and their results underscored the urgent need for air pollution abatement in Beijing or similar polluted megacities and city clusters [19]. Extensive studies have been conducted in recent years to characterize severe haze pollution [20-22]. However, most of them were focused on pollution episodes, an individual season or specific seasons for comparisons (e.g., summer vs. winter; heating vs. non-heating season).

Recent studies have shown that radiocarbon (^{14}C) measurements can unambiguously determine fossil and non-fossil sources of carbonaceous particles, because ^{14}C is completely depleted in fossil-fuel emissions due to its age (half-life 5730 years), whereas non-fossil carbon sources (e.g. biomass burning, cooking or biogenic emissions) show a contemporary ^{14}C content [23, 24]. Moreover, a better ^{14}C-based source apportionment can be obtained when ^{14}C determinations are performed on OC, EC and water-soluble OC [23, 25-28]. Biomass burning, coal combustion, vehicle emission, cooking, and the secondary formation from anthropogenic and biogenic precursors have been identified as important sources of

fine particle in Beijing [21, 29-35]. Recent applications of the positive matrix factorization (PMF) algorithm with aerosol mass spectrometer measurement (AMS-PMF) from field campaigns have revealed a predominance of oxygenated organic aerosol (OOA) over hydrocarbon-like OA (HOA) in various atmospheric environments, although their fossil/non-fossil sources still remain relatively unknown [2, 34-37].

It should be noted that most of these aerosol mass spectrometer studies have been conducted for PM1. A full yearly variation of relative fossil and non-fossil contribution of different carbonaceous aerosols in PM1 in Beijing is urgently needed. To the best of our knowledge, this study is the first time that ^{14}C-based source apportionment of PM1 is simultaneously carried out in different carbonaceous fractions during four seasons in Beijing to attain a comprehensive picture of the source and formation information of carbonaceous aerosols. In addition, ^{14}C results were also combined with AMS-PMF results to quantify the fossil and non-fossil contributions to oxygenated organic carbon (OOC, a surrogate for SOC) and assess contributions to POC from different sources (cooking, biomass burning, coal combustion, hydrocarbon-like OC). Finally, the dataset is also complemented by previous ^{14}C-based source apportionment studies conducted in urban, rural and remote regions in the Northern Hemisphere to gain an overall picture of the sources of OC aerosols.

2 Experimental

2.1 Sampling

PM1 samples were collected on the rooftop of a two-floor building (8 m a.g.l.)

located at the State Key Laboratory of Atmospheric Boundary Layer Physics and Atmospheric Chemistry (LAPC), Institute of Atmospheric Physics (IAP), Chinese Academy of Sciences in Beijing, China. The samples were collected onto pre-baked quartz fibre filters (Pallflex) by a gravimetric volume sampler (Zambelli, Italy) at a flow rate of 38.7 L min^{-1} for around three days for each sample from 28 July 2013 to 21 April 2014. For each season, 10-15 samples were collected. Blank was collected during each season with the pump off during the sampling. The filters were previously enveloped with aluminum foils and then baked at 450 °C for 6 hours before sampling. After sampling, each filter was packed separately stored in a refrigerator under –20°C until the analysis.

2.2 Thermal-optical carbon analysis

OC and EC mass concentrations were measured by the NIOSH thermal-optical transmission (TOT) protocol [38]. The replicate analysis of samples (every 10 samples) showed a good analytical precision with relative standard deviations of 5.2%, 9.5%, and 5.2% for OC, EC and TC, respectively. The average field blank of OC was 1.9±1.0 μg/cm^2 (n=4, equivalent to ~0.3±0.15 μg/m^3), which was subtracted from the measured OC concentrations. A corresponding EC blank was not detectable.

2.3 ^{14}C analysis of the carbonaceous fractions

One to three sequent filter samples were pooled together for ^{14}C measurement. The method of ^{14}C measurement of carbonaceous aerosols was described elsewhere [13, 39, 40]. In short, ^{14}C of TC was analyzed by coupling of an elemental analyzer (EA)

with a MIni CArbon Dating System (MICADAS) at the University of Bern, Switzerland [41, 42]. ^{14}C analysis of EC was carried out by online coupling the MICADAS with a Sunset Lab OC/EC analyzer [43] where CO_2 evolved from the EC peak is separated after OC was combusted from the filter sample (1.5 cm^2) by TOT Swiss_4S protocol [39]. Two samples with relatively high concentrations for each season were selected for ^{14}C measurements of water-soluble OC (WSOC). The mass and f_M values of WSOC were deduced from subtraction of OC and water-insoluble OC (WIOC) based on mass and isotope-mass balancing. ^{14}C measurement of WIOC was measured under the same conditions as OC after water extraction of the filter [26].

^{14}C results were expressed as fractions of modern (f_M), i.e., the fraction of the $^{14}C/^{12}C$ ratio of the sample related to that of the reference year 1950 [44]. f_M(EC) for each sample was further corrected by EC loss (20±8% on average) during the OC removal steps and possibly positive EC artifact from OC charring (10±6% of EC on average) similar to previous analyses [39, 45]. f_M(TC) was corrected for field blanks. The mean uncertainties of f_M(EC) and f_M(TC) were 5% and 2%, respectively. ^{14}C results in OC (f_M(OC)) were then calculated indirectly according to an isotope mass balance [40]:

$$f_M(OC) = \frac{TC \times f_M(TC) - EC \times f_M(EC)}{TC - EC}$$

The uncertainty of f_M(OC) estimated by this approach is on average 8% obtained from an error propagation and includes all the individual uncertainties of f_M(TC) (2%), f_M(EC) (5%), TC (8%) and EC (25%).

Non-fossil fractions of OC and EC (i.e., f_{NF}(OC) and f_{NF}(EC), respectively) were determined from the f_M values and reference values for pure non-fossil sources:

160 $f_{NF}=f_M(sample)/f_M(REF)$. The estimation of reference values ($f_M(REF)$) have been
161 previously reported in details [26, 39, 46]. $f_M(REF)$ values amount to 1.07±0.04 and
162 1.10±0.05 for OC and EC, respectively by a tree-growth model with a long term
163 $^{14}CO_2$ measurement [47] and by assuming that biomass burning contribution to
164 non-fossil OC and EC is 50±25% and 100%, respectively. It should be noted that the
165 uncertainties of references values of $f_{NF}(ref)$ were relatively small compared to
166 uncertainties from overall source-apportionment calculation. Uncertainties were
167 determined by error propagation of all individual uncertainties including OC and EC
168 mass concentrations, ^{14}C results of OC and EC, $f_M(REF)$ as well as corrections for
169 field blanks, EC recovery and charring. The overall average uncertainties of f_{NF} were
170 estimated as 5% (i.e., ranging from 3% to 7%) for OC and 8% (4% to 12%) for EC.
171 Indeed, blank corrections and EC yield corrections are the most important
172 contributors to the total uncertainties of OC and EC, respectively.

173 **2.4 HR-ToF-AMS operation and PMF**

174 An Aerodyne High-resolution Time-of-Flight Aerosol Mass Spectrometer
175 (HR-ToF-AMS) was deployed at the same location for real-time measurements of
176 non-refractory submicron species, including organic aerosols, sulfate, nitrate,
177 ammonium, and chloride in spring (8–28 March, 2014) and winter (17 December
178 2013 to 17 January, 2014). The detailed setup and operations of the HR-ToF-AMS is
179 given elsewhere [22]. The high-resolution mass spectra were then analyzed to determine
180 the elemental ratios of OA, e.g., organic-mass to organic-carbon (OM/OC) and
181 oxygen-to-carbon (O/C), using the Improved-Ambient method [48], and OC mass was

182 calculated as [OA]/[OM/OC]. Positive matrix factorization (PMF) was performed to
183 high-resolution OA spectra to resolve potential source factors in spring and winter.
184 After careful evaluations of the mass spectral profiles and times series following the
185 procedures described elsewhere [49], six factor solution was chosen for both spring and
186 winter studies, which included a hydrocarbon-like OA (HOA), cooking OA (COA),
187 biomass burning OA (BBOA), coal combustion OA (CCOA), and two oxygenated OA
188 factors, i.e., less oxidized OOA (LO-OOA) and more oxidized OOA (MO-OOA). The
189 OC mass for each factor such as hydrocarbon-like OC (HOC), cooking OC (COC),
190 biomass burning OC (BBOC), coal combustion OC (CCOC), and oxidized OOA
191 (OOC) was calculated by dividing the corresponding OM/OC ratio. A more detailed
192 PMF analysis and data interpretation has been given [22].

193 **2.5 ^{14}C-based source apportionment model**

194 An advanced ^{14}C-based source apportionment model was used to quantify OC
195 and EC from each source, which was achieved by the Latin-Hypercube Sampling
196 (LHS) simulations using the dataset from mass concentrations of OC and EC,
197 estimated primary emission ratios for fossil fuel and biomass burning as well as ^{14}C
198 results (termed as the ^{14}C-LHS method) [40]. In total, four major sources were resolved
199 including EC from fossil and non-fossil sources (EC_{FF} and EC_{NF}, receptively), OC
200 from fossil and non-fossil sources (OC_{FF} and OC_{NF}, receptively). OC_{FF} and OC_{NF}
201 were further apportioned into sub-fractions of fossil-fuel OC from primary (POC_{FF})
202 and secondary organic carbon (SOC_{FF}) and non-fossil OC from primary
203 biomass-burning sources (POC_{BB}) and other non-fossil (ONF) sources (e.g. cooking

and primary/secondary non-fossil OC, OC_{ONF}). The equations for the detailed source apportionment are shown in Table 1. Central (median) values with low and high limits were used as input parameters, and all solutions were included in frequency distributions of possible solutions except those producing negative values.

The median values of $(EC/POC)_{BB}$ amounted to 0.3 with a range from 0.1 (low limit) to 0.5 (high limit), according to composed emission ratios in previous literatures [1, 40, 50]. The $(EC/POC)_{FF}$ values were calculated as $(EC/POC)_{FF} = EC_{FF}/(HOC+CCOC)$. Individual HOC and CCOC values were obtained from the AMS-PMF method (see Sec. 2.4). For the samples without AMS-PMF data, a seasonal mean of $(EC/POC)_{FF}$ associated with an uncertainty of 30% was used, which amounted to 0.69 (0.48-0.89) and 1.25 (0.87-1.62) for wintertime and springtime samples, respectively. For samples collected during the autumn, $(EC/POC)_{FF}$ was assumed to be equal to that in spring. In summer, due to decreased contribution from coal combustion to fossil-fuel emissions as previously reported in Beijing [51], a higher $(EC/POC)_{FF}$ of 1.9 (1.3-2.5) was used. This was slightly smaller than EC/OC emission ratios (2.1) from vehicle emission used in our previous study, which were taken from the tunnel experiments in Europe (Gelencsér et al., 2007) and China [52, 53]. The uncertainties and sensitivity test of source apportionment results were carried out by the LHS methodology by generating 10000 sets of inputs used in calculations (see Table 1) [40]. Simulations with negative solutions were not included in final results and the 50^{th} percentiles (or median) of the solution were considered as the best estimate, and the uncertainties were the 10^{th} and 90^{th} percentiles of the solutions.

3 Results and discussion

3.1 OC and EC mass concentrations

As shown in Figure 1, the annual average mass concentrations of OC and EC were 10.1 μg m^{-3} (ranging from 1.9 to 33.8 μg m^{-3}) and 3.8 μg m^{-3} (1.3 to 9.4 μg m^{-3}), respectively. OC mass concentrations were less than those for $PM_{2.5}$ samples in Beijing during 2000 (i.e., 21 μg m^{-3}) and 2013/2014 (i.e., 14.0 ± 11.7 μg/m^3) [33, 54], whereas EC values were comparable to those reported previously (i.e., 3 μg m^{-3}) [33, 54]. The relatively lower OC mass concentrations in PM1 than PM2.5 is likely due to substantial contribution to PM2.5 from larger particles such as dust and primary biogenic emissions [55]. The annual concentrations of OC and EC in PM1 have been only reported in a few studies, and the concentrations in Beijing were significantly higher than those in Elche, Spain (i.e., OC: 3.7±1.3 μg m^{-3}; EC: 1.5±0.6 μg m^{-3}) [56], Brno, the Czech Republic (i.e., OC: 5.8 μg m^{-3}; EC: 1.6 μg m^{-3}) [57] and Taipei (i.e., OC:1.7 μg m^{-3}; EC: 0.8μg m^{-3}) [58] but lower than those in Xi'an (i.e., OC: 21.0 μg m^{-3}; EC: 5.1 μg m^{-3}), China [59]. The seasonal variations of OC and EC were characterized by the lowest mass concentrations in summer with a small standard derivation and the relatively higher values in other three seasons with much larger variations. As illustrated in Figure 1, both relatively high and low values in OC and EC concentrations could be occasionally observed in autumn, winter and spring although their average values were in the following order: winter=spring>autumn. It is very interesting to note that both OC and EC concentrations were very low during a long holiday season (30th Jan to 11th Feb 2014) for the Chinese Spring Festival, which was due to a large decrease in anthropogenic source emissions, e.g., traffic and cooking emissions. Such a "holiday effect" has been also reported in Beijing for 2013 [60]. Similar lower organic aerosols and/or EC concentrations in summer than in the other seasons were also observed previously in Beijing, which was associated with relatively high wet scavenging effects and convection due to abundant precipitation and high temperature, respectively [34, 51]. The overall higher concentrations of carbonaceous aerosols in other seasons were mainly due to combined and complex

effects such as increasing emissions from local and regional-transported coal and biomass/bio-fuel combustion and associated secondary formation as well as unfavorable metrological conditions for pollution dispersions. The relative fossil and non-fossil contributions to OC and EC will be discussed in the following sections.

3.2 Fossil and non-fossil sources of OC and EC

Carbonaceous aerosol was divided into the following four categories: OC from fossil and non-fossil sources, i.e., OC_{FF} and OC_{NF}, and EC from fossil and non-fossil (or biomass-burning) sources, i.e., EC_{FF} and EC_{NF} (i.e., $EC_{NF} = EC_{BB}$) (see Section 2.5). Annual-average biomass -burning contribution to EC was 18±7% with a range of 4% to 33%, suggesting a dominant contribution of fossil-fuel combustion to EC in Beijing rather than non-fossil sources. Fossil fraction in EC reported here was larger than those estimated by bottom-up inventories (i.e., 61±7%) in China [61]. Such a high annual-average fossil fraction in EC is consistent with the results reported in Beijing (i.e., 79%± 6%), China [51], Jeju Island, Korea (i.e., 76 ± 11%) [13], and Ningbo, China (i.e., 77±15%) [27], but was remarkably higher than those found in South Asia such as Hanimaadhoo, Maldives (i.e., 47±9%) and Sinhagad, India (49±8%) [17] as well as a background site in South China (62±11%) [18] where local/regional biomass burning contribution was found to be more important than fossil fuel combustion. The biomass-burning fraction in EC was the lowest in summer (7%) and increased to around 20% during the rest of the year due to increased residential and/or open biomass-burning emissions, which was in line with a previous study for larger particles (e.g., PM4.3) in Beijing during 2010/2011. As shown Figure 2b, fossil-derived EC was a substantial contribution of TC in summer with a mean

278 contribution of 39±3%, significantly higher than those in autumn (23±5%), winter
279 (19±2%) and spring (19±2%).

280 Non-fossil contribution to OC ranged from 28% to 75% with a mean of
281 52%±12%, which is exclusively larger than the corresponding contribution to EC
282 (Figure 2a). This is due to relatively high contribution to OC from primary and
283 secondary formation from non-fossil emissions such as biogenic, cooking and
284 biomass-burning sources compared to EC. OC was dominated by non-fossil sources
285 throughout the year except winter when a higher fossil-derived contribution for both
286 absolute mass concentration (i.e., 8.0±5.2 μg m^{-3}) and relative fraction (i.e., 59±6%)
287 was observed. The highest fossil-derived OC in winter was associated with enhanced
288 coal combustions for heating during the cold periods in North China [51, 55].
289 Interestingly, fossil fraction in EC was not higher in winter than in autumn and spring,
290 suggesting that source pattern was not changed significantly during these three
291 seasons.

292 However, the secondary formation from fossil-derived precursors may become
293 more important and this would actually increase the fossil fraction in OC (see the next
294 section). Indeed, the importance of SOC formation from fossil-fuel source has been
295 previously identified in winter of Beijing and a downwind site of North China [13, 21, 40].
296 In contrast to fossil-derived OC, mass concentrations and relative contributions of
297 non-fossil OC were higher during autumn and spring, which was very likely due to
298 enhanced biomass-burning. The lowest non-fossil OC was observed in summer,
299 although secondary production from biogenic emissions should be higher in this

season with relatively high temperature and strong solar radiation [13], and the overall low mass concentration was likely due to strong atmospheric convection and dispersion as explained above. The seasonal trend of the TC sources was very similar to that of OC but with a relatively lower non-fossil contribution, suggesting that total carbonaceous aerosols are largely controlled by OC emissions and formation processes.

3.3 Primary and secondary organic carbon

OC contributions from POC_{BB}, OC_{ONF}, POC_{FF}, SOC_{FF} sources are displayed in Figure 3. In order to present data variability, the best estimates (the median values) as well as 10^{th}, 25^{th}, 75^{th} and 90^{th} percentiles from the LHS simulations are also shown. On a yearly basis, the most important contributor of OC was $OC_{ONF,}$ i.e., all other non-fossil sources (i.e., 33%±11% for OC_{ONF}) excluding primary biomass-burning OC (POC_{BB}), mainly comprising primary and secondary biogenic OC as well as cooking OC. The highest OC_{ONF} contribution in summer was due to the increasing contributions from primary biogenic emissions and associated SOC formation with favorable atmospheric conditions (i.e., high temperature and solar radiation) as well as reduced emission for heating. OC_{ONF} contribution became lowest in winter because biogenic OC in sub-micron aerosols should be negligible or very small in the cold periods in North China. The mean OC_{ONF} contribution (22±9%) in winter may be used as a upper limit of cooking OC, which was comparable to results resolved from AMS-PMF (~20% for COC/OC in winter, see Figure 4) in our study and also cooking contribution to organic aerosols (19±4%) previously reported in Beijing [14]. The

remaining OC was shared by fossil-derived POC (29±4%), primary biomass-burning OC (22±11%) and fossil-derived SOC (15±4%). For fossil-fuel derived OC, primary emissions dominated over secondary formation in almost all cases.

A clear seasonal variation of biomass-burning source was observed with the highest contribution in autumn (27±13%) and spring (26±14%), followed by winter (19±10%) and summer (16±9%). The enhanced biomass-burning activities in autumn in Beijing and other areas in Northeast China have also been reported by measurements of biomass-burning markers such as levoglucosan and K^+ as well as stable carbon isotopic composition, which can be attributed to agricultural waste and/or fallen leaves burning [62, 63]. POC_{FF} contributions were significantly higher in summer and winter. A large fraction of POC_{FF} could be from vehicle emissions elucidated by a lower mean OC_{FF}/EC_{FF} ratio in summer (i.e., mean: 0.6; range: 0.5-0.7) compared to other seasons (i.e., mean: 1.70; range: 0.5-3.8). In winter, the enhancement was observed for both the POC_{FF} (33±4%) and SOC_{FF} (26±10%) contributions, associated with increasing emissions from coal combustion for heating. However, the SOC contribution in PM1 samples was obviously lower than those reported for a severe haze episode across East China in winter 2013 [40], implying relatively larger SOC contribution to PM2.5 than PM1.

To further investigate the relative contributions of biomass burning, cooking emissions and secondary formation to non-fossil OC, ^{14}C-based source apportionment results were integrated with AMS-PMF results. Average mass concentrations of OC determined by filter-based OC/EC analyzer and on-line AMS methods (OC-AMS) are

shown in Figure 4. Due to analytical uncertainties in either method, a mean OC-AMS/OC-Sunset ratio was 1.1±0.2, and such a difference was also reported in other studies [37, 64]. In the following, only relative contributions from each source to OC were compared to remove possible influences from differences in absolute concentrations (Figure 4). In spring and winter of Beijing, non-fossil OC was mostly derived from cooking and biomass-burning emissions. OOC, a proxy for secondary OC, comprised only a minor non-fossil fraction (15%). The results suggest that SOC was dominated by fossil fuel emissions in Beijing at least in these two seasons.

It should be noted that BBOC resolved from the AMS-PMF approach was smaller than POC_{BB} obtained from the ^{14}C-LHS method. The difference between the AMS-PMF and ^{14}C-LHS results can be explained by the uncertainties in both methods. Biomass-burning contribution may be underestimated by the AMS-PMF if aged BBOC was not included in the PMF model when biomass-burning OA was subject to substantial aging during regional transport. It may also be possible that POC_{BB} was overestimated by the ^{14}C method if a too low $(EC/POC)_{BB}$ was used in the LHS calculation, which was also reported during the DAURE campaign in Northeast Spain [64]. With a combination approach with ^{14}C and AMS-PMF methods, coal combustion was estimated to account for 62% and 56% of fossil-derived POC in winter and spring, respectively, implying an overall importance of coal combustion to OC aerosol in Beijing. The biogenic/biomass-burning derived SOC (i.e., estimated as OOC_{NF}) contributions accounted for 7% and 9% of OC in Beijing during winter and spring, respectively, demonstrating that OC was dominated by anthropogenic emissions

including biomass burning, cooking emissions as well as primary and secondary OC from fossil-fuel emissions.

3.4 Fossil and non-fossil sources of WSOC and WIOC

WSOC can be directly emitted as primary particles mainly from biomass burning or produced as secondary organic aerosol (SOA) [65-67]. Ambient studies provide evidence that SOA produced through the oxidation of volatile organic compounds (VOCs) followed by gas-to-particle conversion contains more polar compounds and thus may be a more important source of WSOC [66-69] compared to primary organic aerosols. WSOC is therefore thought to be a good proxy of secondary organic carbon (SOC) in the absence of biomass burning [67]. The average WSOC/OC ratio in our study was 0.53±0.19 (ranging from 0.21 to 0.84). And WSOC/OC mass concentration ratio and non-fossil fraction of OC (i.e., $f_{NF}(OC)$) show a very similar temporal variation (Figure 5) with a good correlation ($r=0.60$, $p<0.05$), indicating that non-fossil source was an important contributor of WSOC. To confirm this hypothesis, ^{14}C measurement was also performed on sub-fractions of OC including WSOC and water-insoluble OC (WIOC) of two samples for each season. Based on these measurements, the WSOC concentrations from non-fossil sources ($WSOC_{NF}$) ranged from 0.6 to 7.6 μg/m^3, whereas the corresponding range for WSOC from fossil-fuel emissions ($WSOC_{FF}$) was 0.5 to 11.6 μg/m^3. Non-fossil sources were major if not dominate contributors of WSOC for nearly all studied samples with a mean contribution of 58%±9% (Figure 6). The only exception (i.e., $f_{NF}(WSOC)=0.39$) was the aerosol sample collected from 2013/12/2 to 2013/12/26 when the highest OC concentration during the whole sampling periods was observed. The highest fossil source contribution was also found for the WIOC fraction (i.e., $f_{NF}(WIOC)=0.31$) for the same sample. These results showed that during this haze episode, fossil emission was the most important source of OC. $WSOC_{NF}$ can be further apportioned to WSOC from biomass burning (i.e., $WSOC_{BB}$) and non-fossil SOC (i.e., $WSOC_{NF,SOC}$):

$$WSOCNF=WSOC_{NF,SOC}+WSOC_{BB}$$

$WSOC_{BB}=POC_{BB}*(WSOC/OC)_{BB}$

where POC_{BB} was previously estimated (see Sec.3.3). SOC-to-OC emission ratios of biomass burning (i.e., $(WSOC/OC)_{BB}$) is assigned as 0.8±0.2 (ranging from 0.6 to 1.0) in this study according to observations of different biomass types around the world [65, 70]. Therefore, primary biomass burning and non-fossil derived SOC accounted for 62%±17% and 38%±17% of $WSOC_{NF}$, respectively. This suggest that biomass burning was generally a major contributor of non-fossil WSOC in Beijing. Furthermore, $WSOC_{FF}$ was significantly correlated ($r=0.94$, $p<0.01$) with SOC_{FF} (see Sec. 3.3), suggesting that an importance contribution of fossil-derived SOC to $WSOC_{FF}$. On the yearly-basis, non-fossil contributions to WSOC were larger than those to WIOC (Figure 6), although most of the data is not statistically significant from the 1:1 line and some opposite cases were also found occasionally. Similar observations were published for other locations in Asia [71], Europe [26] and the USA [72], which is due to relatively high water solubility of major sources of WSOC such as biomass-burning OC and SOC that are composed of a large fraction of polar and highly oxygenated compounds [70, 73, 74].

4 Implications

Despite dominant fossil-fuel contribution to EC particles due to large emissions from traffic and coal combustion, our study demonstrates that non-fossil emissions are generally a dominant contributor of OC including WIOC and WSOC fractions in a heavily polluted megacity in China. Such an important non-fossil contribution to OC agrees with source information identified in OC aerosols obtained in the Northern Hemisphere at urban, rural, semi-urban, and background sites in Asia, Europe and USA (Figure 7). The ^{14}C-based source apportionment database shows a mean non-fossil fraction of 68±13% across all sites (Figure 7). ^{14}C results of EC/TC/WSOC were not compiled for the comparisons since these carbonaceous fractions cannot

420 fully represent OC aerosols. As discussed in the previous section, WSOC/OC ratios
421 and non-fossil contribution of OC in Beijing have very similar temporal variations,
422 indicating that biomass-burning emissions and biogenic-derived SOC formation were
423 very important contributors of non-fossil OC. Indeed, WSOC/OC ratios may be also
424 increased due to organic aerosol aging during regional and/or long-range transport, so
425 it can be anticipated that the regional-transported non-fossil OC from rural sites to
426 urban areas would also increase non-fossil OC fraction in urban regions. As shown in
427 Figure 7, fossil contribution is apparently higher in the USA (i.e., with fossil
428 contribution of 44±11%) and East Asia (i.e., 39±13%) than those observed in Europe
429 (i.e., 25±9%). This may be because most ^{14}C-based studies in the USA and East Asia
430 have been conducted within, near and downwind of urban areas. Furthermore, wood
431 burning emissions have recently become a more important contributor of European
432 aerosols. This would be especially the case in winter, decreasing fossil contribution.
433 This study shows that a combined approach of AMS-PMF and ^{14}C methods
434 provide more comprehensive picture of the source and formation information of
435 carbonaceous aerosols than either method alone. Therefore, such approaches are
436 recommended to be used as a routine basis in a long-term monitoring network (e.g. at
437 supersites) for a better source apportionment. Our study also provides a direct
438 evidence that non-fossil source plays a major role in organic aerosol concentrations
439 not only in rural/remote areas but also in many polluted urban sites, which seems to
440 be contrasting to the fact that fossil fuel emissions (e.g., coal combustion and vehicle
441 exhaust) often dominate EC aerosols (i.e., an excellent marker for primary

carbonaceous aerosols) in urban areas. This unexpectedly high non-fossil contribution to OC in urban areas may be explained by urban non-fossil carbon emissions (e.g. cooking emissions and associated SOA), regional transported or locally season-dependent biomass burning emissions [75, 76], as well as biogenic/biomass-burning SOA linked with complex and combined atmospheric mechanisms such as enhancement by anthropogenic emissions [77].

Notes

The authors declare no competing financial interest.

Acknowledgment

This work was supported by the National Natural Science Foundation of China (Grant Nos. 91644103, 41603104, 41475117, 41571130024, 41575120), the Strategic Priority Research Program (B) of the Chinese Academy of Sciences (Grant No. XDB05030306), and the Startup Foundation for Introducing Talent of NUIST (No. 2015r023 and 2015r019) as well as Thousand Youth Talents Plan of China.

References

1. Gelencsér, A.; May, B.; Simpson, D.; Sánchez-Ochoa, A.; Kasper-Giebl, A.; Puxbaum, H.; Caseiro, A.; Pio, C.; Legrand, M., Source apportionment of PM2.5 organic aerosol over Europe: Primary/secondary, natural/anthropogenic, and fossil/biogenic origin. *J. Geophys. Res.* **2007,** *112*, (D23), D23S04.

2. Jimenez, J. L.; Canagaratna, M. R.; Donahue, N. M.; Prevot, A. S. H.; Zhang, Q.; Kroll, J. H.; DeCarlo, P. F.; Allan, J. D.; Coe, H.; Ng, N. L.; Aiken, A. C.; Docherty, K. S.; Ulbrich, I. M.; Grieshop, A. P.; Robinson, A. L.; Duplissy, J.; Smith, J. D.; Wilson, K. R.; Lanz, V. A.; Hueglin, C.; Sun, Y. L.; Tian, J.; Laaksonen, A.; Raatikainen, T.; Rautiainen, J.; Vaattovaara, P.; Ehn, M.; Kulmala, M.; Tomlinson, J. M.; Collins, D. R.; Cubison, M. J.; Dunlea, E. J.; Huffman, J. A.; Onasch, T. B.; Alfarra, M. R.; Williams, P. I.; Bower, K.; Kondo, Y.; Schneider, J.; Drewnick, F.; Borrmann, S.; Weimer, S.; Demerjian, K.; Salcedo, D.; Cottrell,

L.; Griffin, R.; Takami, A.; Miyoshi, T.; Hatakeyama, S.; Shimono, A.; Sun, J. Y.; Zhang, Y. M.; Dzepina, K.; Kimmel, J. R.; Sueper, D.; Jayne, J. T.; Herndon, S. C.; Trimborn, A. M.; Williams, L. R.; Wood, E. C.; Middlebrook, A. M.; Kolb, C. E.; Baltensperger, U.; Worsnop, D. R., Evolution of organic aerosols in the atmosphere. *Science* **2009,** *326*, (5959), 1525-1529.

3. Mauderly, J. L.; Chow, J. C., Health effects of organic aerosols. *Inhalation Toxicol.* **2008,** *20*, (3), 257-288.

4. Highwood, E. J.; Kinnersley, R. P., When smoke gets in our eyes: The multiple impacts of atmospheric black carbon on climate, air quality and health. *Environ. Int.* **2006,** *32*, (4), 560-566.

5. IPCC, *Climate change 2013: The physical science basis. contribution of working group I to the fifth assessment report of the intergovernmental panel on climate change*. Cambridge University Press: Cambridge, United Kingdom and New York, NY, USA, 2013; p 1533.

6. Pöschl, U., Atmospheric aerosols: composition, transformation, climate and health effects. *Angew. Chem., Int. Ed.* **2005,** *44*, (46), 7520-40.

7. Lighty, J. S.; Veranth, J. M.; Sarofim, A. F., Combustion aerosols: Factors governing their size and composition and implications to human health. *J. Air Waste Manage. Assoc.* **2000,** *50*, (9), 1565-1618.

8. Hallquist, M.; Wenger, J. C.; Baltensperger, U.; Rudich, Y.; Simpson, D.; Claeys, M.; Dommen, J.; Donahue, N. M.; George, C.; Goldstein, A. H.; Hamilton, J. F.; Herrmann, H.; Hoffmann, T.; Iinuma, Y.; Jang, M.; Jenkin, M. E.; Jimenez, J. L.; Kiendler-Scharr, A.; Maenhaut, W.; McFiggans, G.; Mentel, T. F.; Monod, A.; Prevot, A. S. H.; Seinfeld, J. H.; Surratt, J. D.; Szmigielski, R.; Wildt, J., The formation, properties and impact of secondary organic aerosol: current and emerging issues. *Atmos. Chem. Phys.* **2009,** *9*, (14), 5155-5236.

9. Fuzzi, S.; Andreae, M. O.; Huebert, B. J.; Kulmala, M.; Bond, T. C.; Boy, M.; Doherty, S. J.; Guenther, A.; Kanakidou, M.; Kawamura, K.; Kerminen, V. M.; Lohmann, U.; Russell, L. M.; Poschl, U., Critical assessment of the current state of scientific knowledge, terminology, and research needs concerning the role of organic aerosols in the atmosphere, climate, and global change. *Atmos. Chem. Phys.* **2006,** *6*, 2017-2038.

10. Zhang, Y. L.; Kawamura, K.; Cao, F.; Lee, M., Stable carbon isotopic compositions of low-molecular-weight dicarboxylic acids, oxocarboxylic acids, α-dicarbonyls, and fatty acids: Implications for atmospheric processing of organic aerosols. *J. Geophys. Res.* **2016,** *121*, (7), 3707-3717.

11. Bond, T. C.; Doherty, S. J.; Fahey, D. W.; Forster, P. M.; Berntsen, T.; DeAngelo, B. J.; Flanner, M. G.; Ghan, S.; Karcher, B.; Koch, D.; Kinne, S.; Kondo, Y.; Quinn, P. K.; Sarofim, M. C.; Schultz, M. G.; Schulz, M.; Venkataraman, C.; Zhang, H.; Zhang, S.; Bellouin, N.; Guttikunda, S. K.; Hopke, P. K.; Jacobson, M. Z.; Kaiser, J. W.; Klimont, Z.; Lohmann, U.; Schwarz, J. P.; Shindell, D.; Storelvmo, T.; Warren, S. G.; Zender, C. S., Bounding the role of black carbon in the climate system: A scientific assessment. *J. Geophys. Res.* **2013,** *118*, (11), 5380-5552.

12. Carlton, A. G.; Wiedinmyer, C.; Kroll, J. H., A review of Secondary Organic Aerosol (SOA) formation from isoprene. *Atmos. Chem. Phys.* **2009,** *9*, (14), 4987-5005.

13. Zhang, Y. L.; Kawamura, K.; Agrios, K.; Lee, M.; Salazar, G.; Szidat, S., Fossil and

Nonfossil Sources of Organic and Elemental Carbon Aerosols in the Outflow from Northeast China. *Environ. Sci. Technol.* **2016,** *50*, (12), 6284-92.

14. Hu, W.; Hu, M.; Hu, W.; Jimenez, J. L.; Yuan, B.; Chen, W.; Wang, M.; Wu, Y.; Chen, C.; Wang, Z.; Peng, J.; Zeng, L.; Shao, M., Chemical composition, sources, and aging process of submicron aerosols in Beijing: Contrast between summer and winter. *J. Geophys. Res.* **2016,** *121*, (4), 1955-1977.

15. Bond, T. C.; Streets, D. G.; Yarber, K. F.; Nelson, S. M.; Woo, J. H.; Klimont, Z., A technology-based global inventory of black and organic carbon emissions from combustion. *J. Geophys. Res.* **2004,** *109*, (D14), D14203.

16. Streets, D. G.; Bond, T. C.; Lee, T.; Jang, C., On the future of carbonaceous aerosol emissions. *J. Geophys. Res.* **2004,** *109*, (D24), D24212.

17. Sheesley, R. J.; Kirillova, E.; Andersson, A.; Krusa, M.; Praveen, P. S.; Budhavant, K.; Safai, P. D.; Rao, P. S. P.; Gustafsson, O., Year-round radiocarbon-based source apportionment of carbonaceous aerosols at two background sites in South Asia. *J. Geophys. Res.* **2012,** *117*, Artn D10202.

18. Zhang, Y.-L.; Li, J.; Zhang, G.; Zotter, P.; Huang, R.-J.; Tang, J.-H.; Wacker, L.; Prévôt, A. S. H.; Szidat, S., Radiocarbon-based source apportionment of carbonaceous aerosols at a regional background site on hainan Island, South China. *Environ. Sci. Technol.* **2014,** *48*, (5), 2651-2659.

19. Zheng, S.; Pozzer, A.; Cao, C. X.; Lelieveld, J., Long-term (2001–2012) concentrations of fine particulate matter (PM_{2.5}) and the impact on human health in Beijing, China. *Atmos. Chem. Phys.* **2015,** *15*, (10), 5715-5725.

20. Guo, S.; Hu, M.; Zamora, M. L.; Peng, J.; Shang, D.; Zheng, J.; Du, Z.; Wu, Z.; Shao, M.; Zeng, L.; Molina, M. J.; Zhang, R., Elucidating severe urban haze formation in China. *Proc. Nat. Acad. Sci. U.S.A.* **2014,** *111*, (49), 17373-8.

21. Huang, R. J.; Zhang, Y.; Bozzetti, C.; Ho, K. F.; Cao, J. J.; Han, Y.; Daellenbach, K. R.; Slowik, J. G.; Platt, S. M.; Canonaco, F.; Zotter, P.; Wolf, R.; Pieber, S. M.; Bruns, E. A.; Crippa, M.; Ciarelli, G.; Piazzalunga, A.; Schwikowski, M.; Abbaszade, G.; Schnelle-Kreis, J.; Zimmermann, R.; An, Z.; Szidat, S.; Baltensperger, U.; El Haddad, I.; Prevot, A. S., High secondary aerosol contribution to particulate pollution during haze events in China. *Nature* **2014,** *514*, (7521), 218-22.

22. Sun, Y. L.; Du, W.; Fu, P. Q.; Wang, Q. Q.; Li, J.; Ge, X. L.; Zhang, Q.; Zhu, C. M.; Ren, L. J.; Xu, W. Q.; Zhao, J.; Han, T. T.; Worsnop, D. R.; Wang, Z. F., Primary and secondary aerosols in Beijing in winter: sources, variations and processes. *Atmos. Chem. Phys.* **2016,** *16*, (13), 8309-8329.

23. Szidat, S., Sources of Asian haze. *Science* **2009,** *323*, (5913), 470-471.

24. Heal, M., The application of carbon-14 analyses to the source apportionment of atmospheric carbonaceous particulate matter: a review. *Anal. Bioanal. Chem.* **2014,** *406*, (1), 81-98.

25. Szidat, S.; Jenk, T. M.; Synal, H.-A.; Kalberer, M.; Wacker, L.; Hajdas, I.; Kasper-Giebl, A.; Baltensperger, U., Contributions of fossil fuel, biomass-burning, and biogenic emissions to carbonaceous aerosols in Zurich as traced by ^{14}C. *J. Geophys. Res.* **2006,** *111*, (D7), D07206.

26. Zhang, Y. L.; Zotter, P.; Perron, N.; Prévôt, A. S. H.; Wacker, L.; Szidat, S., Fossil and

555 non-fossil sources of different carbonaceous fractions in fine and coarse particles by
556 radiocarbon measurement. *Radiocarbon* **2013,** *55*, (2-3), 1510-1520.
557 27. Liu, D.; Li, J.; Zhang, Y.; Xu, Y.; Liu, X.; Ding, P.; Shen, C.; Chen, Y.; Tian, C.; Zhang,
558 G., The use of levoglucosan and radiocarbon for source apportionment of $PM_{2.5}$ carbonaceous
559 aerosols at a background site in East China. *Environ. Sci. Technol.* **2013,** *47*, (18), 10454-61.
560 28. Bernardoni, V.; Calzolai, G.; Chiari, M.; Fedi, M.; Lucarelli, F.; Nava, S.; Piazzalunga,
561 A.; Riccobono, F.; Taccetti, F.; Valli, G.; Vecchi, R., Radiocarbon analysis on organic and
562 elemental carbon in aerosol samples and source apportionment at an urban site in Northern
563 Italy. *J. Aerosol Sci.* **2013,** *56*, 88-99.
564 29. Zhang, J. K.; Sun, Y.; Liu, Z. R.; Ji, D. S.; Hu, B.; Liu, Q.; Wang, Y. S., Characterization
565 of submicron aerosols during a month of serious pollution in Beijing, 2013. *Atmos. Chem.*
566 *Phys.* **2014,** *14*, (6), 2887-2903.
567 30. Zhao, P. S.; Dong, F.; He, D.; Zhao, X. J.; Zhang, X. L.; Zhang, W. Z.; Yao, Q.; Liu, H. Y.,
568 Characteristics of concentrations and chemical compositions for PM2.5 in the region of
569 Beijing, Tianjin, and Hebei, China. *Atmos. Chem. Phys.* **2013,** *13*, (9), 4631-4644.
570 31. Yang, F.; Tan, J.; Zhao, Q.; Du, Z.; He, K.; Ma, Y.; Duan, F.; Chen, G.; Zhao, Q.,
571 Characteristics of $PM_{2.5}$ speciation in representative megacities and across China. *Atmos.*
572 *Chem. Phys.* **2011,** *11*, (11), 5207-5219.
573 32. Wang, Q.; Shao, M.; Zhang, Y.; Wei, Y.; Hu, M.; Guo, S., Source apportionment of fine
574 organic aerosols in Beijing. *Atmos. Chem. Phys.* **2009,** *9*, (21), 8573-8585.
575 33. Zheng, M.; Salmon, L. G.; Schauer, J. J.; Zeng, L. M.; Kiang, C. S.; Zhang, Y. H.; Cass,
576 G. R., Seasonal trends in PM2.5 source contributions in Beijing, China. *Atmos. Environ.* **2005,**
577 *39*, (22), 3967-3976.
578 34. Sun, Y. L.; Wang, Z. F.; Du, W.; Zhang, Q.; Wang, Q. Q.; Fu, P. Q.; Pan, X. L.; Li, J.;
579 Jayne, J.; Worsnop, D. R., Long-term real-time measurements of aerosol particle composition
580 in Beijing, China: seasonal variations, meteorological effects, and source analysis. *Atmos.*
581 *Chem. Phys.* **2015,** *15*, (17), 10149-10165.
582 35. Sun, Y. L.; Jiang, Q.; Wang, Z. F.; Fu, P. Q.; Li, J.; Yang, T.; Yin, Y., Investigation of the
583 sources and evolution processes of severe haze pollution in Beijing in January 2013. *J.*
584 *Geophys. Res.* **2014,** *119*, (7), 4380-4398.
585 36. Zhang, Q.; Jimenez, J. L.; Canagaratna, M. R.; Allan, J. D.; Coe, H.; Ulbrich, I.; Alfarra,
586 M. R.; Takami, A.; Middlebrook, A. M.; Sun, Y. L.; Dzepina, K.; Dunlea, E.; Docherty, K.;
587 DeCarlo, P. F.; Salcedo, D.; Onasch, T.; Jayne, J. T.; Miyoshi, T.; Shimono, A.; Hatakeyama,
588 S.; Takegawa, N.; Kondo, Y.; Schneider, J.; Drewnick, F.; Borrmann, S.; Weimer, S.;
589 Demerjian, K.; Williams, P.; Bower, K.; Bahreini, R.; Cottrell, L.; Griffin, R. J.; Rautiainen, J.;
590 Sun, J. Y.; Zhang, Y. M.; Worsnop, D. R., Ubiquity and dominance of oxygenated species in
591 organic aerosols in anthropogenically-influenced Northern Hemisphere midlatitudes. *Geophys.*
592 *Res. Lett.* **2007,** *34*, (13), L13801.
593 37. Zotter, P.; El-Haddad, I.; Zhang, Y.; Hayes, P. L.; Zhang, X.; Lin, Y.-H.; Wacker, L.;
594 Schnelle-Kreis, J.; Abbaszade, G.; Zimmermann, R.; Surratt, J. D.; Weber, R.; Jimenez, J. L.;
595 Szidat, S.; Baltensperger, U.; Prévôt, A. S. H., Diurnal cycle of fossil and nonfossil carbon
596 using radiocarbon analyses during CalNex. *J. Geophys. Res.* **2014,** *119*, (11), 6818-6835.
597 38. Birch, M. E.; Cary, R. A., Elemental carbon-based method for monitoring occupational
598 exposures to particulate diesel exhaust. *Aerosol Sci. Technol.* **1996,** *25*, (3), 221-241.

39. Zhang, Y. L.; Perron, N.; Ciobanu, V. G.; Zotter, P.; Minguillón, M. C.; Wacker, L.; Prévôt, A. S. H.; Baltensperger, U.; Szidat, S., On the isolation of OC and EC and the optimal strategy of radiocarbon-based source apportionment of carbonaceous aerosols. *Atmos. Chem. Phys.* **2012,** *12*, 10841-10856.
40. Zhang, Y. L.; Huang, R. J.; El Haddad, I.; Ho, K. F.; Cao, J. J.; Han, Y.; Zotter, P.; Bozzetti, C.; Daellenbach, K. R.; Canonaco, F.; Slowik, J. G.; Salazar, G.; Schwikowski, M.; Schnelle-Kreis, J.; Abbaszade, G.; Zimmermann, R.; Baltensperger, U.; Prévôt, A. S. H.; Szidat, S., Fossil vs. non-fossil sources of fine carbonaceous aerosols in four Chinese cities during the extreme winter haze episode of 2013. *Atmos. Chem. Phys.* **2015,** *15*, (3), 1299-1312.
41. Salazar, G.; Zhang, Y. L.; Agrios, K.; Szidat, S., Development of a method for fast and automatic radiocarbon measurement of aerosol samples by online coupling of an elemental analyzer with a MICADAS AMS. *Nucl. Instr. and Meth. in Phys. Res. B.* **2015,** *361*, 163-167.
42. Szidat, S.; Salazar, G. A.; Vogel, E.; Battaglia, M.; Wacker, L.; Synal, H. A.; Turler, A., C-14 Analysis and Sample Preparation at the New Bern Laboratory for the Analysis of Radiocarbon with Ams (Lara). *Radiocarbon* **2014,** *56*, (2), 561-566.
43. Agrios, K.; Salazar, G.; Zhang, Y.-L.; Uglietti, C.; Battaglia, M.; Luginbühl, M.; Ciobanu, V. G.; Vonwiller, M.; Szidat, S., Online coupling of pure O2 thermo-optical methods – 14C AMS for source apportionment of carbonaceous aerosols. *Nucl. Instr. and Meth. in Phys. Res. B.* **2015,** *361*, 288-293.
44. Stuiver, M.; Polach, H. A., Discussion: Reporting of 14C data. *Radiocarbon* **1977,** *19*, (3), 355-363.
45. Zotter, P.; Ciobanu, V. G.; Zhang, Y. L.; El-Haddad, I.; Macchia, M.; Daellenbach, K. R.; Salazar, G. A.; Huang, R. J.; Wacker, L.; Hueglin, C.; Piazzalunga, A.; Fermo, P.; Schwikowski, M.; Baltensperger, U.; Szidat, S.; Prévôt, A. S. H., Radiocarbon analysis of elemental and organic carbon in Switzerland during winter-smog episodes from 2008 to 2012 – Part 1: Source apportionment and spatial variability. *Atmos. Chem. Phys.* **2014,** *14*, (24), 13551-13570.
46. Minguillón, M. C.; Perron, N.; Querol, X.; Szidat, S.; Fahrni, S. M.; Alastuey, A.; Jimenez, J. L.; Mohr, C.; Ortega, A. M.; Day, D. A.; Lanz, V. A.; Wacker, L.; Reche, C.; Cusack, M.; Amato, F.; Kiss, G.; Hoffer, A.; Decesari, S.; Moretti, F.; Hillamo, R.; Teinila, K.; Seco, R.; Penuelas, J.; Metzger, A.; Schallhart, S.; Muller, M.; Hansel, A.; Burkhart, J. F.; Baltensperger, U.; Prevot, A. S. H., Fossil versus contemporary sources of fine elemental and organic carbonaceous particulate matter during the DAURE campaign in Northeast Spain. *Atmos. Chem. Phys.* **2011,** *11*, (23), 12067-12084.
47. Mohn, J.; Szidat, S.; Fellner, J.; Rechberger, H.; Quartier, R.; Buchmann, B.; Emmenegger, L., Determination of biogenic and fossil CO_2 emitted by waste incineration based on $^{14}CO_2$ and mass balances. *Bioresour. Technol.* **2008,** *99*, (14), 6471-6479.
48. Canagaratna, M. R.; Jimenez, J. L.; Kroll, J. H.; Chen, Q.; Kessler, S. H.; Massoli, P.; Hildebrandt Ruiz, L.; Fortner, E.; Williams, L. R.; Wilson, K. R.; Surratt, J. D.; Donahue, N. M.; Jayne, J. T.; Worsnop, D. R., Elemental ratio measurements of organic compounds using aerosol mass spectrometry: characterization, improved calibration, and implications. *Atmos. Chem. Phys.* **2015,** *15*, (1), 253-272.
49. Zhang, Q.; Jimenez, J. L.; Canagaratna, M. R.; Ulbrich, I. M.; Ng, N. L.; Worsnop, D. R.;

643 Sun, Y. L., Understanding atmospheric organic aerosols via factor analysis of aerosol mass
644 spectrometry: a review. *Anal. Bioanal. Chem.* **2011,** *401*, (10), 3045-3067.
645 50. Genberg, J.; Hyder, M.; Stenström, K.; Bergström, R.; Simpson, D.; Fors, E.; Jönsson, J.
646 Å.; Swietlicki, E., Source apportionment of carbonaceous aerosol in southern Sweden. *Atmos.*
647 *Chem. Phys.* **2011,** *11*, (22), 11387-11400.
648 51. Zhang, Y.-L.; Schnelle-Kreis, J. r.; Abbaszade, G. l.; Zimmermann, R.; Zotter, P.; Shen,
649 R.-r.; Schäfer, K.; Shao, L.; Prévôt, A. S. H.; Szidat, S. n., Source apportionment of elemental
650 carbon in Beijing, China: Insights from radiocarbon and organic marker measurements.
651 *Environ. Sci. Technol.* **2015,** *49*, (14), 8408-8415.
652 52. Huang, X. F.; Yu, J. Z.; He, L. Y.; Hu, M., Size distribution characteristics of elemental
653 carbon emitted from Chinese vehicles: Results of a tunnel study and atmospheric implications.
654 *Environ. Sci. Technol.* **2006,** *40*, (17), 5355-5360.
655 53. He, L. Y.; Hu, M.; Zhang, Y. H.; Huang, X. F.; Yao, T. T., Fine particle emissions from
656 on-road vehicles in the Zhujiang Tunnel, China. *Environ. Sci. Technol.* **2008,** *42*, (12),
657 4461-4466.
658 54. Ji, D.; Zhang, J.; He, J.; Wang, X.; Pang, B.; Liu, Z.; Wang, L.; Wang, Y., Characteristics
659 of atmospheric organic and elemental carbon aerosols in urban Beijing, China. *Atmos.*
660 *Environ.* **2016,** *125, Part A*, 293-306.
661 55. Elser, M.; Huang, R. J.; Wolf, R.; Slowik, J. G.; Wang, Q.; Canonaco, F.; Li, G.; Bozzetti,
662 C.; Daellenbach, K. R.; Huang, Y.; Zhang, R.; Li, Z.; Cao, J.; Baltensperger, U.; El-Haddad, I.;
663 Prévôt, A. S. H., New insights into PM2.5 chemical composition and sources in two major
664 cities in China during extreme haze events using aerosol mass spectrometry. *Atmos. Chem.*
665 *Phys.* **2016,** *16*, (5), 3207-3225.
666 56. Yubero, E.; Galindo, N.; Nicolás, J. F.; Crespo, J.; Calzolai, G.; Lucarelli, F., Temporal
667 variations of PM1 major components in an urban street canyon. *Environmental Science and*
668 *Pollution Research* **2015,** *22*, (17), 13328-13335.
669 57. Křůmal, K.; Mikuška, P.; Večeřa, Z., Polycyclic aromatic hydrocarbons and hopanes in
670 PM1 aerosols in urban areas. *Atmos. Environ.* **2013,** *67*, 27-37.
671 58. Cheung, H. C.; Chou, C. C. K.; Chen, M. J.; Huang, W. R.; Huang, S. H.; Tsai, C. Y.; Lee,
672 C. S. L., Seasonal variations of ultra-fine and submicron aerosols in Taipei, Taiwan:
673 implications for particle formation processes in a subtropical urban area. *Atmos. Chem. Phys.*
674 **2016,** *16*, (3), 1317-1330.
675 59. Shen, Z.; Cao, J.; Arimoto, R.; Han, Y.; Zhu, C.; Tian, J.; Liu, S., Chemical
676 Characteristics of Fine Particles (PM1) from Xi'an, China. *Aerosol Sci. Technol.* **2010,** *44*, (6),
677 461-472.
678 60. Jiang, Q.; Sun, Y. L.; Wang, Z.; Yin, Y., Aerosol composition and sources during the
679 Chinese Spring Festival: fireworks, secondary aerosol, and holiday effects. *Atmos. Chem.*
680 *Phys.* **2015,** *15*, (11), 6023-6034.
681 61. Chen, B.; Andersson, A.; Lee, M.; Kirillova, E. N.; Xiao, Q.; Krusa, M.; Shi, M.; Hu, K.;
682 Lu, Z.; Streets, D. G.; Du, K.; Gustafsson, O., Source forensics of black carbon aerosols from
683 China. *Environ. Sci. Technol.* **2013,** *47*, (16), 9102-8.
684 62. Zhang, T.; Claeys, M.; Cachier, H.; Dong, S. P.; Wang, W.; Maenhaut, W.; Liu, X. D.,
685 Identification and estimation of the biomass burning contribution to Beijing aerosol using
686 levoglucosan as a molecular marker. *Atmos. Environ.* **2008,** *42*, (29), 7013-7021.

687 63. Cao, F.; Zhang, S. C.; Kawamura, K.; Zhang, Y. L., Inorganic markers, carbonaceous
688 components and stable carbon isotope from biomass burning aerosols in Northeast China. *Sci.*
689 *Total Environ.* **2016,** *572*, 1244-1251.
690 64. Minguillon, M. C.; Perron, N.; Querol, X.; Szidat, S.; Fahrni, S. M.; Alastuey, A.;
691 Jimenez, J. L.; Mohr, C.; Ortega, A. M.; Day, D. A.; Lanz, V. A.; Wacker, L.; Reche, C.;
692 Cusack, M.; Amato, F.; Kiss, G.; Hoffer, A.; Decesari, S.; Moretti, F.; Hillamo, R.; Teinila, K.;
693 Seco, R.; Penuelas, J.; Metzger, A.; Schallhart, S.; Muller, M.; Hansel, A.; Burkhart, J. F.;
694 Baltensperger, U.; Prevot, A. S. H., Fossil versus contemporary sources of fine elemental and
695 organic carbonaceous particulate matter during the DAURE campaign in Northeast Spain.
696 *Atmos. Chem. Phys.* **2011,** *11*, (23), 12067-12084.
697 65. Sannigrahi, P.; Sullivan, A. P.; Weber, R. J.; Ingall, E. D., Characterization of
698 water-soluble organic carbon in urban atmospheric aerosols using solid-state C-13 NMR
699 spectroscopy. *Environ. Sci. Technol.* **2006,** *40*, (3), 666-672.
700 66. Kondo, Y.; Miyazaki, Y.; Takegawa, N.; Miyakawa, T.; Weber, R. J.; Jimenez, J. L.;
701 Zhang, Q.; Worsnop, D. R., Oxygenated and water-soluble organic aerosols in Tokyo. *J.*
702 *Geophys. Res.* **2007,** *112*, (D1), D01203.
703 67. Weber, R. J.; Sullivan, A. P.; Peltier, R. E.; Russell, A.; Yan, B.; Zheng, M.; de Gouw, J.;
704 Warneke, C.; Brock, C.; Holloway, J. S.; Atlas, E. L.; Edgerton, E., A study of secondary
705 organic aerosol formation in the anthropogenic-influenced southeastern United States. *J.*
706 *Geophys. Res.* **2007,** *112*, (D13), D13302.
707 68. Miyazaki, Y.; Kondo, Y.; Takegawa, N.; Komazaki, Y.; Fukuda, M.; Kawamura, K.;
708 Mochida, M.; Okuzawa, K.; Weber, R. J., Time-resolved measurements of water-soluble
709 organic carbon in Tokyo. *J. Geophys. Res.* **2006,** *111*, (D23), D23206.
710 69. Hecobian, A.; Zhang, X.; Zheng, M.; Frank, N.; Edgerton, E. S.; Weber, R. J.,
711 Water-Soluble Organic Aerosol material and the light-absorption characteristics of aqueous
712 extracts measured over the Southeastern United States. *Atmos. Chem. Phys.* **2010,** *10*, (13),
713 5965-5977.
714 70. Mayol-Bracero, O. L.; Guyon, P.; Graham, B.; Roberts, G.; Andreae, M. O.; Decesari, S.;
715 Facchini, M. C.; Fuzzi, S.; Artaxo, P., Water-soluble organic compounds in biomass burning
716 aerosols over Amazonia - 2. Apportionment of the chemical composition and importance of
717 the polyacidic fraction. *J. Geophys. Res.* **2002,** *107*, (D20), D8091.
718 71. Kirillova, E. N.; Andersson, A.; Sheesley, R. J.; Kruså, M.; Praveen, P. S.; Budhavant, K.;
719 Safai, P. D.; Rao, P. S. P.; Gustafsson, Ö., ^{13}C and ^{14}C-based study of sources and atmospheric
720 processing of water-soluble organic carbon (WSOC) in South Asian aerosols. *J. Geophys. Res.*
721 **2013,** *118*, (2), 614-626.
722 72. Wozniak, A. S.; Bauer, J. E.; Dickhut, R. M., Characteristics of water-soluble organic
723 carbon associated with aerosol particles in the eastern United States. *Atmos. Environ.* **2012,**
724 *46*, 181-188.
725 73. Sullivan, A. P.; Frank, N.; Kenski, D. M.; Collett, J. L., Application of high-performance
726 anion-exchange chromatography-pulsed amperometric detection for measuring carbohydrates
727 in routine daily filter samples collected by a national network: 2. Examination of sugar
728 alcohols/polyols, sugars, and anhydrosugars in the upper Midwest. *J. Geophys. Res.* **2011,** *116*,
729 D08303.
730 74. Noziere, B.; Kalberer, M.; Claeys, M.; Allan, J.; D'Anna, B.; Decesari, S.; Finessi, E.;

731 Glasius, M.; Grgic, I.; Hamilton, J. F.; Hoffmann, T.; Iinuma, Y.; Jaoui, M.; Kahnt, A.; Kampf,
732 C. J.; Kourtchev, I.; Maenhaut, W.; Marsden, N.; Saarikoski, S.; Schnelle-Kreis, J.; Surratt, J.
733 D.; Szidat, S.; Szmigielski, R.; Wisthaler, A., The molecular identification of organic
734 compounds in the atmosphere: state of the art and challenges. *Chem Rev* **2015,** *115*, (10),
735 3919-83.
736 75. Cheng, Y.; Engling, G.; He, K. B.; Duan, F. K.; Ma, Y. L.; Du, Z. Y.; Liu, J. M.; Zheng,
737 M.; Weber, R. J., Biomass burning contribution to Beijing aerosol. *Atmos. Chem. Phys.* **2013,**
738 *13*, (15), 7765-7781.
739 76. Yan, C.; Zheng, M.; Bosch, C.; Andersson, A.; Desyaterik, Y.; Sullivan, A. P.; Collett, J.
740 L.; Zhao, B.; Wang, S.; He, K.; Gustafsson, O., Important fossil source contribution to brown
741 carbon in Beijing during winter. *Sci Rep* **2017,** *7*, 43182.
742 77. Hoyle, C. R.; Boy, M.; Donahue, N. M.; Fry, J. L.; Glasius, M.; Guenther, A.; Hallar, A.
743 G.; Hartz, K. H.; Petters, M. D.; Petaja, T.; Rosenoern, T.; Sullivan, A. P., A review of the
744 anthropogenic influence on biogenic secondary organic aerosol. *Atmos. Chem. Phys.* **2011,** *11*,
745 (1), 321-343.
746 78. Liu, J.; Li, J.; Vonwiller, M.; Liu, D.; Cheng, H.; Shen, K.; Salazar, G.; Agrios, K.; Zhang,
747 Y.; He, Q.; Ding, X.; Zhong, G.; Wang, X.; Szidat, S.; Zhang, G., The importance of
748 non-fossil sources in carbonaceous aerosols in a megacity of central China during the 2013
749 winter haze episode: A source apportionment constrained by radiocarbon and organic tracers.
750 *Atmos. Environ.* **2016,** *144*, 60-68.
751 79. Szidat, S.; Ruff, M.; Perron, N.; Wacker, L.; Synal, H.-A.; Hallquist, M.; Shannigrahi, A.
752 S.; Yttri, K. E.; Dye, C.; Simpson, D., Fossil and non-fossil sources of organic carbon (OC)
753 and elemental carbon (EC) in Goeteborg, Sweden. *Atmos. Chem. Phys.* **2009,** *9*, 1521-1535.
754 80. Wozniak, A. S.; Bauer, J. E.; Dickhut, R. M.; Xu, L.; McNichol, A. P., Isotopic
755 characterization of aerosol organic carbon components over the eastern United States. *J.*
756 *Geophys. Res.* **2012,** *117*, (D13), D13303.
757 81. Dusek, U.; ten Brink, H. M.; Meijer, H. A. J.; Kos, G.; Mrozek, D.; Röckmann, T.;
758 Holzinger, R.; Weijers, E. P., The contribution of fossil sources to the organic aerosol in the
759 Netherlands. *Atmos. Environ.* **2013,** *74*, 169-176.
760 82. Zotter, P.; El-Haddad, I.; Zhang, Y.; Hayes, P. L.; Zhang, X.; Lin, Y. H.; Wacker, L.;
761 Schnelle-Kreis, J.; Abbaszade, G.; Zimmermann, R., Diurnal cycle of fossil and nonfossil
762 carbon using radiocarbon analyses during CalNex. *J. Geophys. Res.* **2014,** *119*, (11),
763 6818-6835.
764 83. Heal, M. R.; Naysmith, P.; Cook, G. T.; Xu, S.; Duran, T. R.; Harrison, R. M.,
765 Application of ^{14}C analyses to source apportionment of carbonaceous PM2.5 in the UK.
766 *Atmos. Environ.* **2011,** *45*, (14), 2341-2348.
767 84. Aiken, a. C.; de Foy, B.; Wiedinmyer, C.; DeCarlo, P. F.; Ulbrich, I. M.; Wehrli, M. N.;
768 Szidat, S.; Prevot, a. S. H.; Noda, J.; Wacker, L.; Volkamer, R.; Fortner, E.; Wang, J.; Laskin,
769 a.; Shutthanandan, V.; Zheng, J.; Zhang, R.; Paredes-Miranda, G.; Arnott, W. P.; Molina, L. T.;
770 Sosa, G.; Querol, X.; Jimenez, J. L., Mexico City aerosol analysis during MILAGRO using
771 high resolution aerosol mass spectrometry at the urban supersite (T0) – Part 2: Analysis of the
772 biomass burning contribution and the modern carbon fraction. **2009,** *9*, 25915-25981.

773 85. Ulevicius, V.; Byčenkienė, S.; Bozzetti, C.; Vlachou, A.; Plauškaitė, K.; Mordas, G.;
774 Dudoitis, V.; Abbaszade, G.; Remeikis, V.; Garbaras, A.; Masalaite, A.; Blees, J.; Fröhlich, R.;
775 Dällenbach, K. R.; Canonaco, F.; Slowik, J. G.; Dommen, J.; Zimmermann, R.;
776 Schnelle-Kreis, J.; Salazar, G. A.; Agrios, K.; Szidat, S.; El Haddad, I.; Prévôt, A. S. H., Fossil
777 and non-fossil source contributions to atmospheric carbonaceous aerosols during extreme
778 spring grassland fires in Eastern Europe. *Atmos. Chem. Phys.* **2016,** *16*, (9), 5513-5529.
779 86. Gilardoni, S.; Vignati, E.; Cavalli, F.; Putaud, J. P.; Larsen, B. R.; Karl, M.; Stenström, K.;
780 Genberg, J.; Henne, S.; Dentener, F., Better constraints on sources of carbonaceous aerosols
781 using a combined ^{14}C–macro tracer analysis in a European rural background site. *Atmos.*
782 *Chem. Phys* **2011,** *11*, 5685-5700.
783 87. Handa, D.; Nakajima, H.; Arakaki, T.; Kumata, H.; Shibata, Y.; Uchida, M., Radiocarbon
784 analysis of BC and OC in PM10 aerosols at Cape Hedo, Okinawa, Japan, during long-range
785 transport events from East Asian countries. *Nucl. Instr. and Meth. in Phys. Res. B*. **2010,** *268*,
786 (7-8), 1125-1128.
787 88. Fushimi, A.; Wagai, R.; Uchida, M.; Hasegawa, S.; Takahashi, K.; Kondo, M.;
788 Hirabayashi, M.; Morino, Y.; Shibata, Y.; Ohara, T.; Kobayashi, S.; Tanabe, K., Radiocarbon
789 (^{14}C) diurnal variations in fine particles at sites downwind from Tokyo, Japan in summer.
790 *Environ. Sci. Technol.* **2011,** *45*, (16), 6784-92.

791

792 **Table 1**. Equations for ^{14}C-based source apportionment model. See Sec 2.5 for the
793 details.

794

Equations
$EC_{NF} = f_{NF}(EC) \times EC$
$EC_{FF} = EC - EC_{NF}$
$OC_{NF} = f_{NF}(OC) \times OC$
$OC_{FF} = OC - OC_{NF}$
$POC_{FF} = EC_{FF} / (EC/POC)_{FF}$
$SOC_{FF} = OC_{FF} - POC_{FF}$
$POC_{BB} = EC_{NF} / (EC/POC)_{BB}$
$OC_{ONF} = OC_{NF} - POC_{BB}$
$OC_{AMS} = OA_{AMS} / (OM/OC)_{AMS}$

795

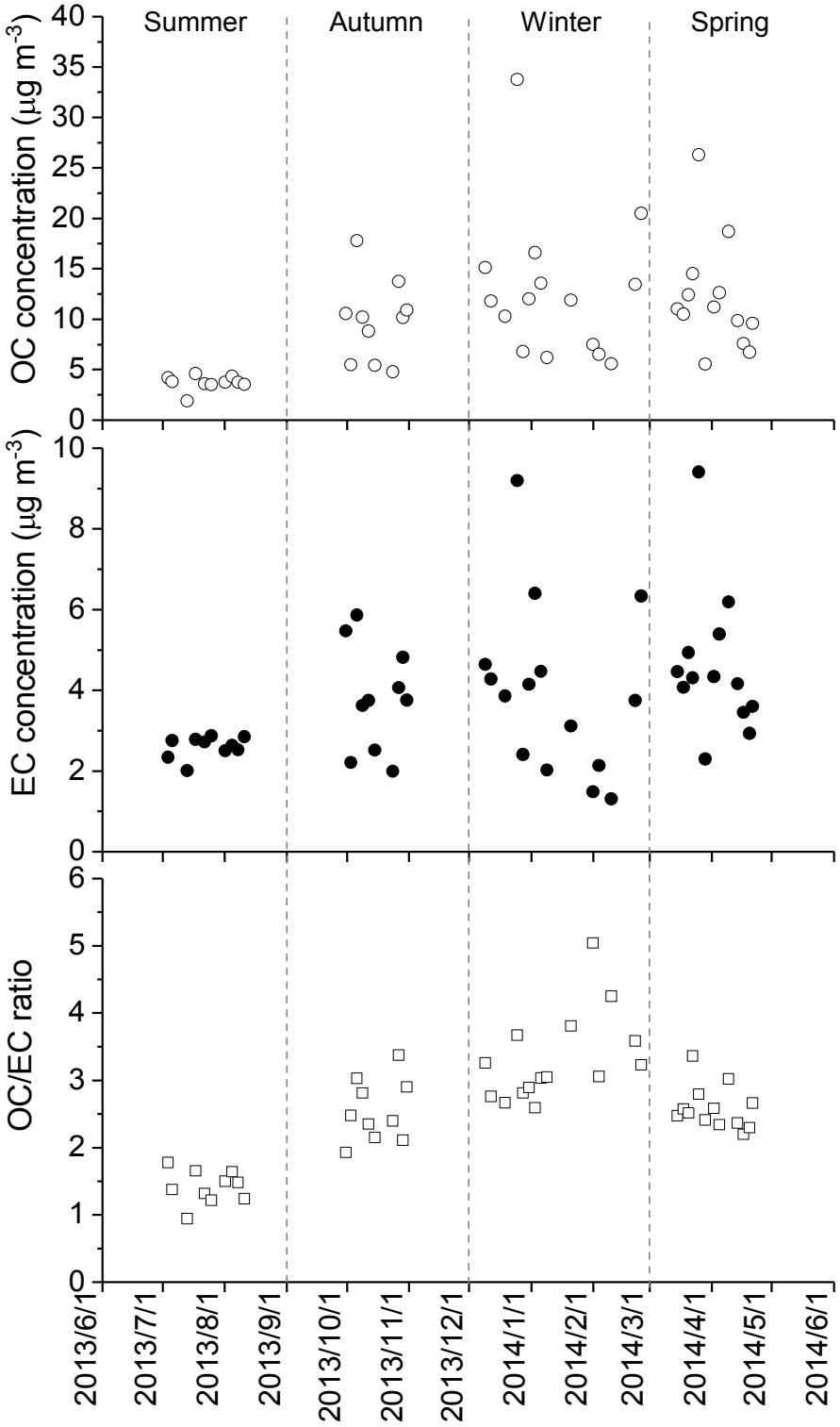

796

797 **Figure 1. Temporal variations of OC and EC mass concentrations as well as**

798 **OC/EC ratio of PM1 samples in Beijing.**

799

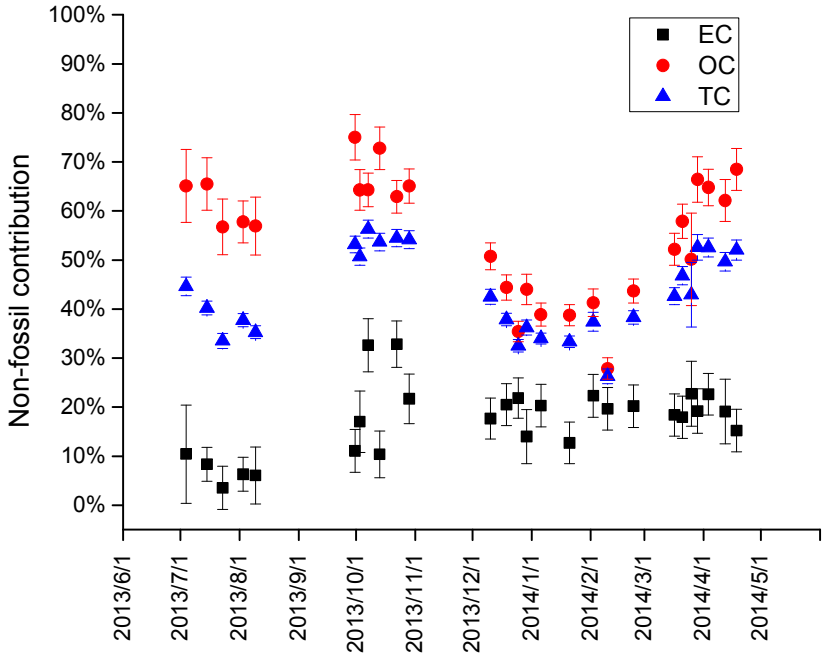

(a)

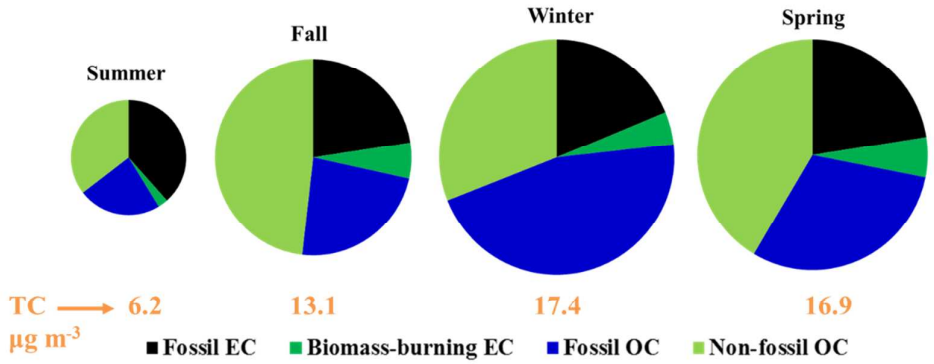

(b)

Figure 2. (a) Temporal variations of non-fossil contribution to OC, EC and TC and (b) average source apportionment results of TC in each season of PM1 samples in Beijing. The numbers below the pie chart represent the average TC concentrations for each season.

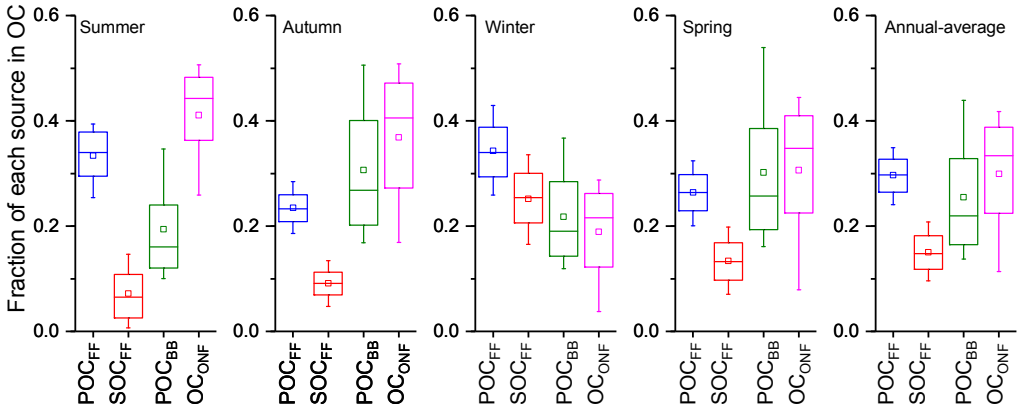

Figure 3. Fractions of each source (i.e., POC_{FF}, SOC_{FF}, POC_{BB}, OC_{ONF}) in OC of PM1 samples in Beijing derived from the Latin-Hypercube Sampling (LHS) simulations for summer, autumn, winter, spring, and the annual-average (from left to right). The box denotes the 25th (lower line), 50th (middle line) and 75th (top line) percentiles; the empty squares within the box denote the mean values; the end of the vertical bars represents the 10th (below the box) and 90th (above the box) percentiles. POC: primary organic carbon, SOC: secondary organic carbon. FF: fossil fuel, NF: non-fossil, ONF: other non-fossil sources (details see the main text).

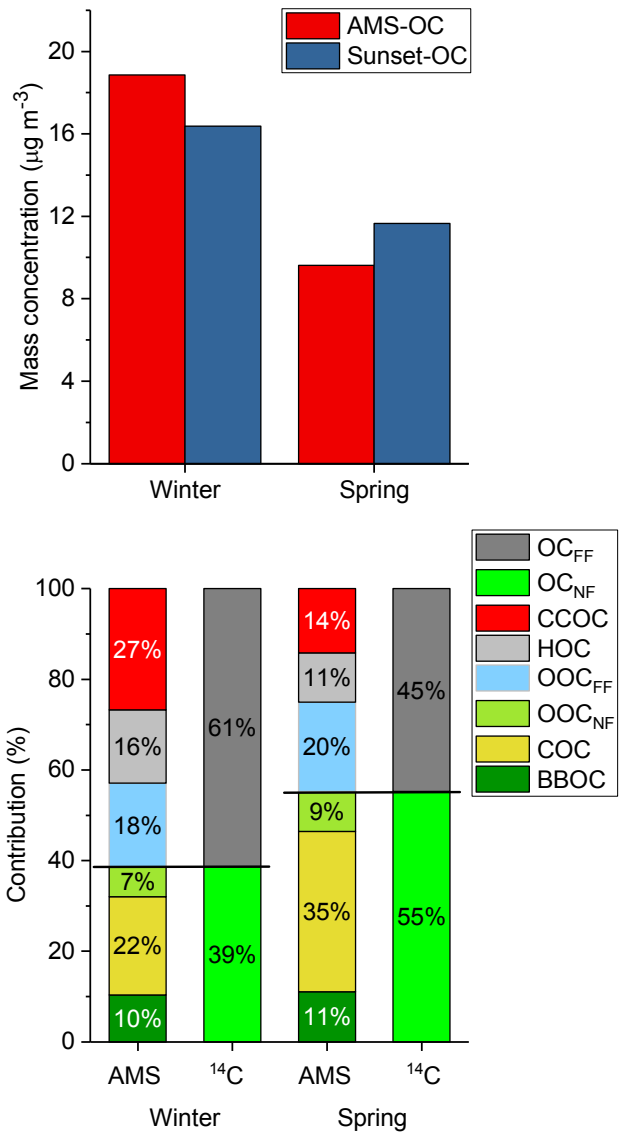

Figure 4. Average mass concentration measured by filter-based Sunset OC/EC analyzer method (OC-Sunset) and AMS method (OC-AMS) during winter (n=4) and spring (n=2) (top) and relative contributions to OC from different sources with a combination of ^{14}C-LHS and AMS-PMF methods (bottom). OC_{FF}: fossil-fuel derived OC; OC_{NF}: non-fossil OC; CCOC: primary coal combustion OC; HOC: hydrocarbon-like OC; OOC_{FF}: fossil-fuel oxygenated OC; OOC_{NF}: non-fossil oxygenated OC; COC: primary cooking OC; BBOC: primary biomass burning OC.

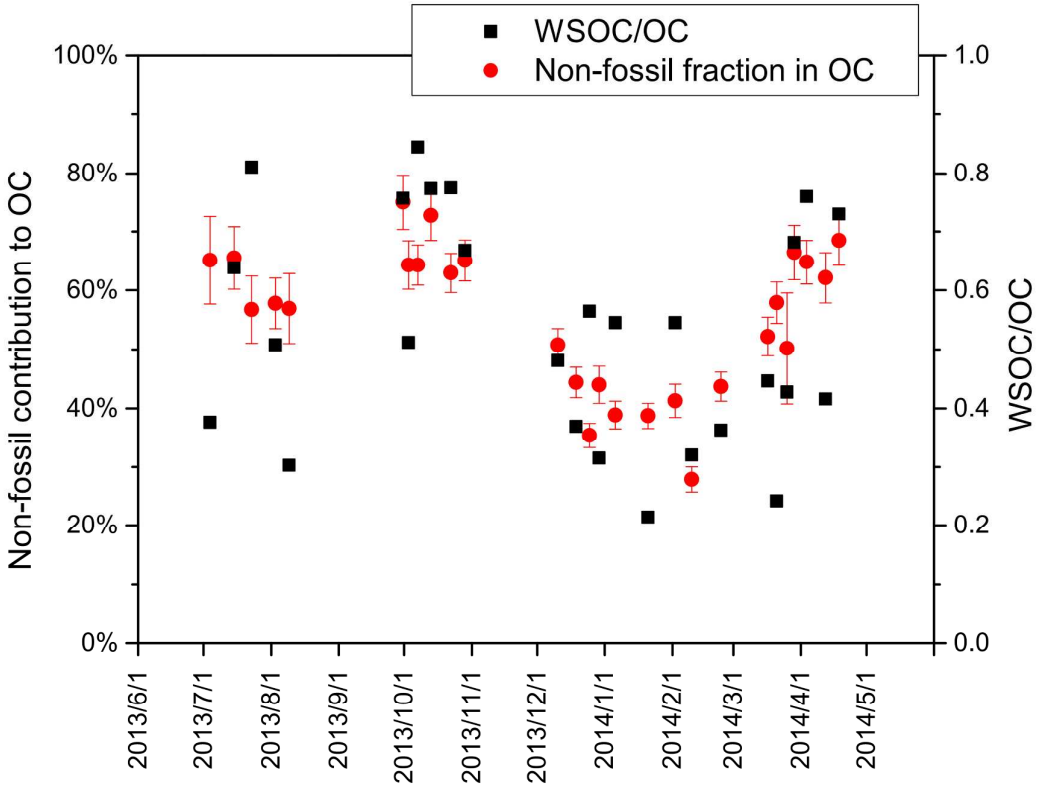

Figure 5. Temporal variations of non-fossil contribution to OC and WSOC/OC ratio of PM_1 samples in Beijing.

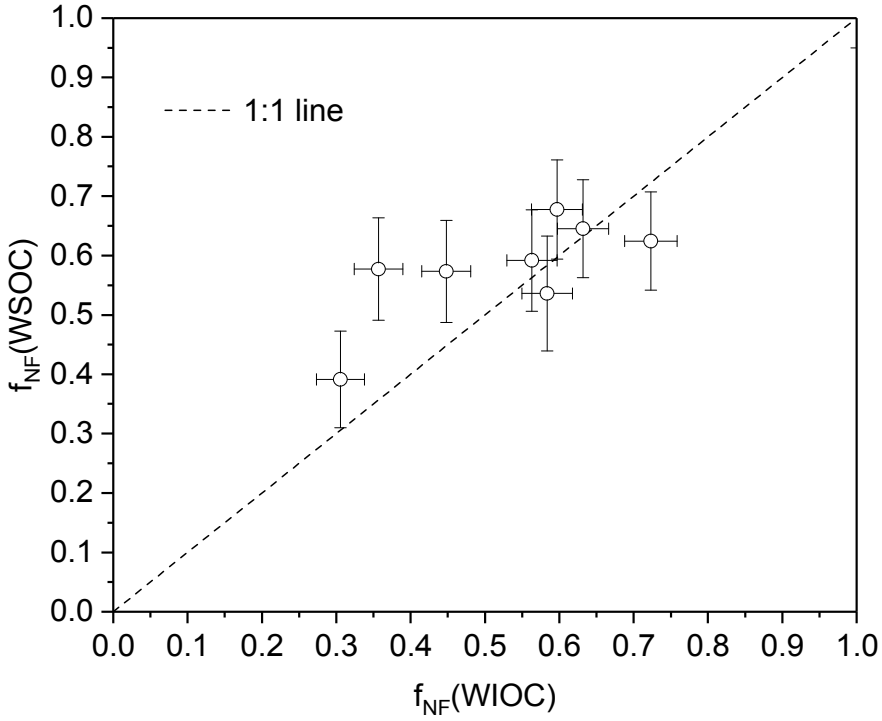

833

834 **Figure 6.** Relationship between f_{NF}(WSOC) and f_{NF}(WIOC).

835

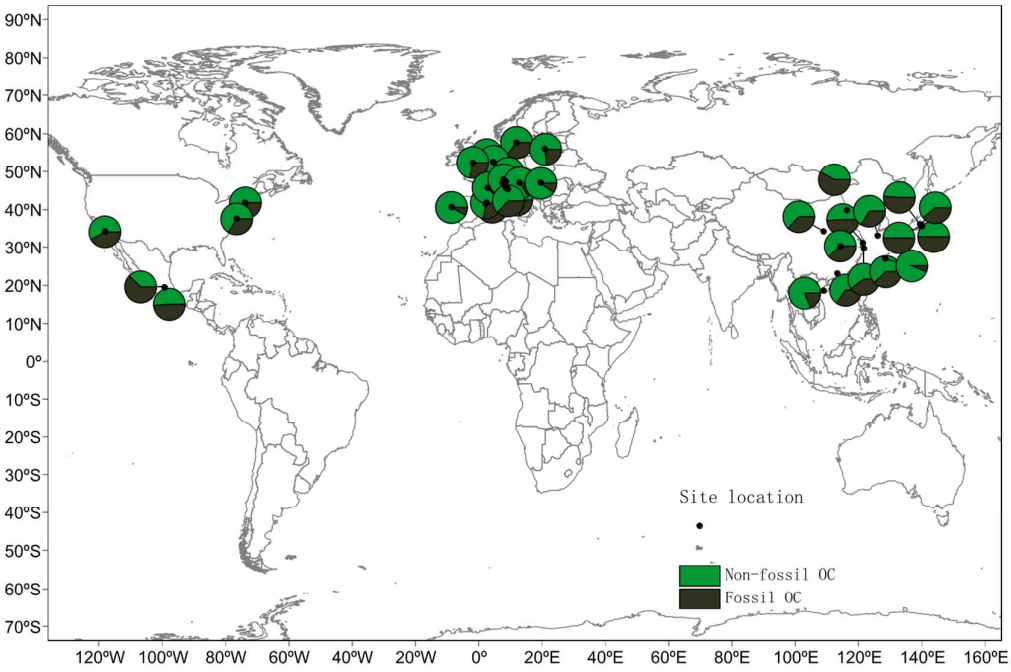

836

837 **Figure 7.** Fossil and non-fossil sources of OC aerosols at different locations around

838 world. The results are obtained from this study and previous ^{14}C-source

839 apportionment studies [1, 13, 18, 26-28, 40, 46, 71, 78-88]. The map is created by MeteoInfo Java

840 Edition 1.3 (http://www.meteothinker.com/).